Beam dynamics of the new LNL injector

A. Pisent

I.N.F.N. Laboratori Nazionali di Legnaro - via Romea, 4 Legnaro (Padova) Italy

Beam dynamics of the new LNL injector.

A.Pisent.

INFN, Laboratori Nazionali di Legnaro

1.INTRODUCTION

The new injector for ALPI will use the positive ion source (ECR), already constructed at LNL[1], and will produce beams of higher intensities and masses respect to what can be done today with the TANDEM. Moreover the construction of a new Experimental Hall (EUROBALL experiment and others) with independent transfer lines allows additional flexibility, since the use of New Injector+ALPI and Tandem beams at the same time by two different experiments will be possible [2].

Due to the higher charge states delivered by the ECR source an RF injector with an equivalent voltage of about 8 MV can substitute the 15 MV XTU Tandem. The Injector consists of Radio Frequency Quadrupole (RFQ) structures up to about 550 keV/u, plus independently phased Quarter Wave Resonators (QWR); this subdivision gives a good acceleration efficiency, allows the use of already developed QWR's and the possibility of a staging in the construction. In Fig. 1 are shown the performances of the ALPI complex injected by the Tandem, directly by the RFQ and by the complete New Injector. Intensities are improved due to the absence of strippers.

Last we mention that this one would be the first superconducting RFQ in operation. The choice is motivated by the need of a CW machine that uses the potentiality of ALPI; most of the experiments done at LNL use high efficiency detectors well matched with beam intensities of some particle nA. For these experiments a machine with half duty cycle and double peak current would not result in the same number of events recorded. Moreover by increasing the number of events grouped in a short time interval (comparable with acquisition time) the number of accidental events grows quadratically. On the other hand in our laboratory there are experiences in superconducting resonators construction and operation, so that this is a natural choice.
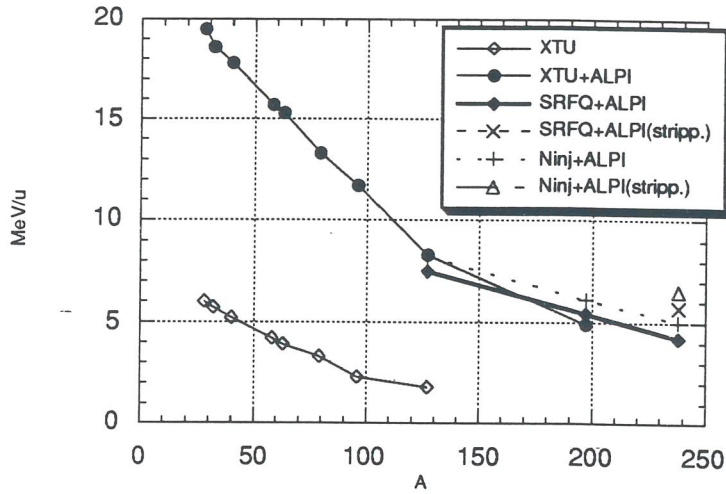
Fig.1 Performances of the LNL accelerators complex under various conditions in the mass vs specific mass diagram: XTU indicates the 15 MV Tandem, ALPI is the complete post accelerator (low and high beta cavities includes), SRFQ represents the two RFQ cavities, NInj indicates the complete injector, including the two QWR cryostats. For the U beam the case with a stripping foil in the middle of ALPI have been calculated, to overcome the Coulomb barrier.

2. RFQ SPECIFICATIONS

In Table I the RFQ specifications are listed. The table is divided between beam specifications and technological constrains.

Table I Specifications.

q/M	28/238	
Energy range	38÷540	keV/u
β range	.009÷.035	
Acceptance (norm)	≥0.8	mm mrad
Output long. emittance	≤0.7	ns keV/u
Surface Field	≤25	MV/m
Stored energy per tank	≤5	J

The RFQ output energy has to be high enough to allow a convenient acceleration in a 80 MHz Quarter Wave Resonator (QWR). The transit time factor in such a structure is in good approximation:

$$TTF = T_0 \sin \frac{\pi}{2} \frac{\beta_0}{\beta}$$

where βc is the particle velocity, $\beta_0 \lambda/2$ is the effective distance between the two accelerating gaps, T_0 is the maximum transit time factor. The bulk Ni QWR's

that are being installed at LNL have $\beta_0=.055$, and with minor modifications $\beta_0=.050$ and $T=0.75\,T_0$ after the RFQ can be achieved [4]. The change of structure (from RFQ to QWR) has the advantage that a set of independently phased resonators can most efficiently accelerate ions with different q/M ratios.

The acceptance considers that typical ion beam emittances from ECR sources, according to CERN, GSI and ANL experiences, are below *0.5 mmmrad*. The longitudinal emittance is kept as small as possible to be competitive with ANL injector.

The maximum electric field that a superconducting surface can stand is function of the material, surface quality, clearness and chemical treatment. The frequency dependence of this value is not as clear as in the case of normal conducting resonators, where the empirical Kilpatrick law can be used. In literature we have found very different values for a Ni surface, up to more than hundred MV/m. Mainly on the basis of the LNL experience with bulk Ni QWR we have fixed our maximum E_s to *25 MV/m* for both the frequency considered during the design work (40 and 80 MHz)[*] .

The maximum stored energy per cavity U has to be limited in a high Q resonator. Actually the required active power to have a Δf feedback control bandwidth is:

$$P_a \;=\; 2\,\pi U * \Delta f.$$

To have routinely a bandwidth of 20 Hz an active power os about 500 W is reqiured. It follows that the total power from the amplifier is 1 kW.

3. DESIGN CRITERIA

As in the design work done in Stony Brook (our starting point) big emphasis is given to the maximization of the acceleration efficiency E_{ff} (energy gain per unit charge per unit length) [5]. Due to this an adiabatic bunching within the RFQ would have made the structure too long, and an external bunching has been chosen (at the expenses of a capture efficiency of about 60%).

Moreover, since we are limited by the maximum surface field E_S , we have to maximize the ratio E_a/E_S :

---

[*] The geometrical factor E_a/E_S for LNL QWRs is around 5; accelerating fields above 5 MV/m have been achieved both with bulk Ni and sputtered Ni resonators.

$$E_a = \frac{E_{ff}}{\cos\phi_s} = V\frac{kA(kR_0, m)}{4}$$

$$E_s = \kappa(kR_0, m)\frac{V}{R_0}$$

$$\frac{E_a}{E_s} = \frac{kR_0 A(kR_0, m)}{4\kappa(kR_0, m)}$$

Here $k=2\pi/\bar{\beta}\lambda$ is the wave number, m is the modulation factor, ratio between the maximum and the minimum vane-beam axis distance, A is the accelerating factor and κ the field enhancement factor.
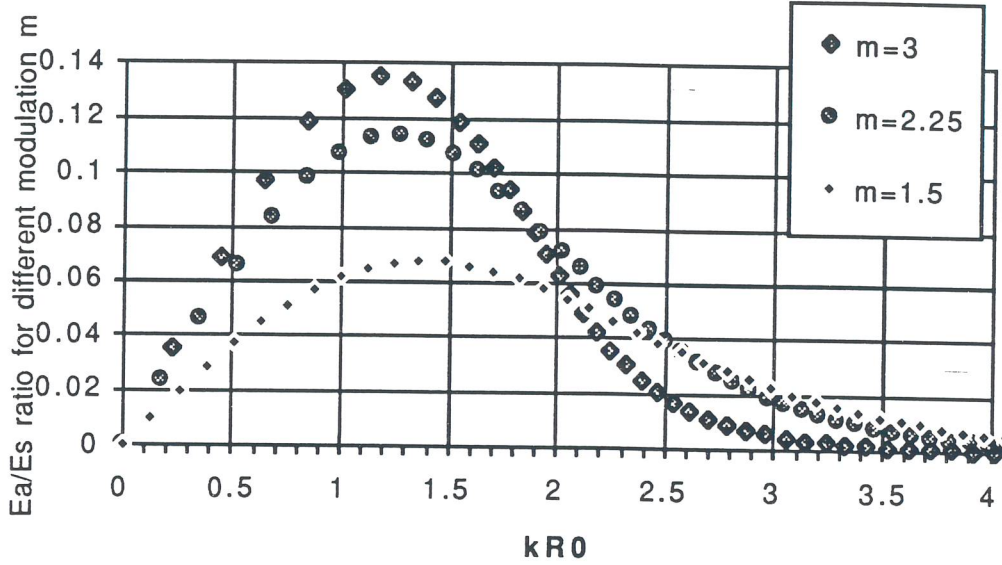

Fig 2. Ratio E_a/E_s as function of kR_0. for different modulation factor m.

The ratio E_a/E_s has, for each m, a maximum as function of kR_0. Using indeed for A the value given by the two terms potential:

$$A(ka, m) = \frac{m^2 - 1}{m^2 I_0(ka) + I_0(mka)}$$

and for the enhancement factor the estimate:

$$\kappa = \sqrt{\frac{q^2}{2} + \left(I_0\left(q\frac{kR_0}{\sqrt{2}}\right)\frac{AkR_0}{2}\right)^2}, \qquad q = 1 + \frac{\rho}{R_0},$$

ρ vanes transverse radius of curvature, one gets the curves of fig. 2 with optimum values for the ratio E_a/E_s around $kR_0 \approx 1.4$ for a wide range of modulation values. Moreover the value of this maximum is a monotonic function of the modulation factor m, but with negative second derivative, i.e. the advantage of high modulations almost saturates, while all kind of exotic

effects related to Bessel functions increase. For this reason we have chosen to remain below *m=3*, even if calculations of accelerating and enhancement factors have been performed up to *m=4* .

The fields E_a and E_s are kept constant if V and R_0 are both proportional to β (stepwise from one tank to the next one). Increasing β the stored energy becomes a problem, since:

$$U = \frac{1}{2} (C / \ell) V^2 \ell$$

and the capacitance per unit length in a quadrupole is not very sensitive to the geometrical details (about 120pF/m).

If we fix kR_0, E_s and U at the beginning of the RFQ, both the average aperture R_0 (that we keep constant) and the maximum RFQ length are fixed. In Fig.3 those two quantities are plotted as a function of the RFQ input energy for different kR_0, and resonant frequency.

Both RFQ too short and R_0, too big (very massive electrodes) are not desirable. It is therefore clear that efficient RFQs cannot have initial energy higher then 500 keV/u (@80 MHz), while the 40 MHz choice, offering higher focusing easier longitudinal dynamics, is very soon limited by stored energy.
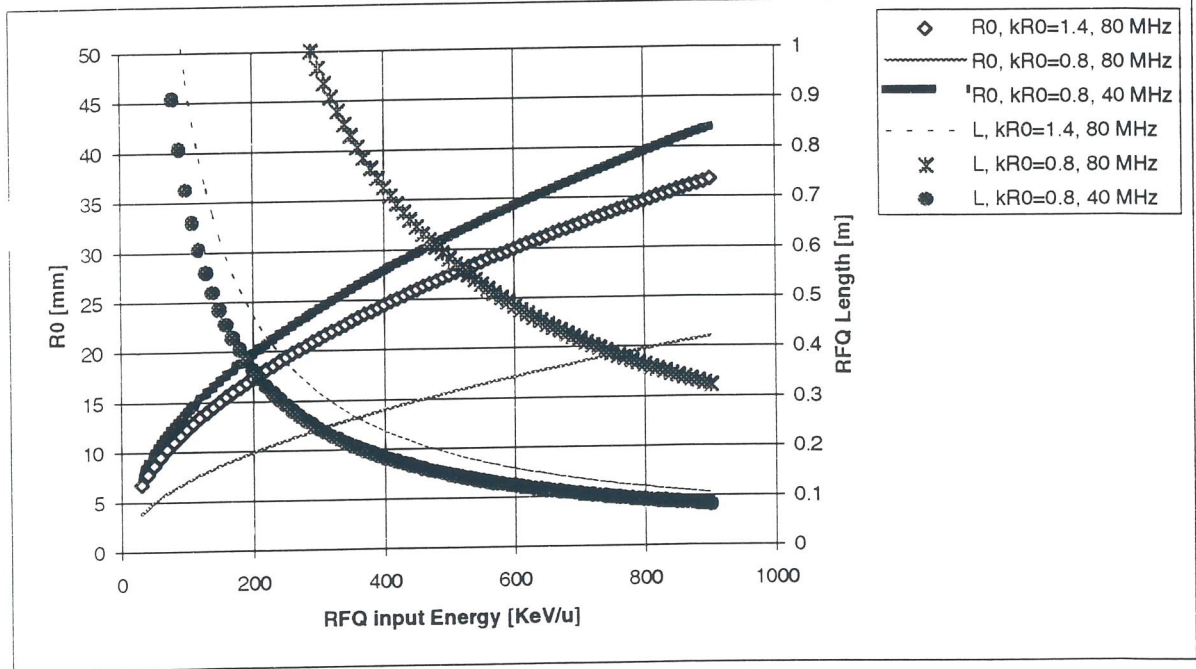

Fig .3 Average aperture R_0 and maximum RFQ length L as a function of the RFQ input energy in the range of the entire New Injector. A stored energy of 4J, surface field 26 MV/m, enhancement factor 1.2, vanes capacitance 120 pF/m are assumed.

Moreover increasing R_0 and the acceleration at the same time the transverse phase advance per period σ_t decreases, with the following consequences:

1. the acceptance is reduced
2. the parametric resonance $\sigma_l = 2\sigma_t$, σ_l longitudinal phase advance, can be met.
3. the jump of σ_t from one RFQ to the next one can cause an important transverse mismatch.

For all these reasons the use of RFQ's above 550 keV/u seems problematic and the transition to QWR's convenient.

4. THE NOMINAL CASE

An effective RFQ accelerator can be obtained by choosing $kR_0 \approx 1.4$ and an high modulation factor; our design value is $m=2.8$ for the linear RFQ, corresponding to $m=3$ taking into account the constant transverse radius geometry. The voltage V is determined by the maximum surface field; the synchronous phase ϕ_s has to leave the required acceptance ($|\phi_s|$ and the RF defocusing must be small enough).

Short RFQ's have higher efficiency and smaller stored energy, but more inter tank drift spaces. These spaces have a physical length $d \approx 200$ mm determined by the hardware and cause a drifting of the transverse ellipsis and beam mismatching in the following RFQ.

At 80 MHz it is convenient to construct two RFQ's: the first relatively long, with small R_0 and V, and a second shorter, with higher R_0, V and E_{ff}. The same optimization criteria brings to 3 RFQ's @40 MHz.

Indeed the sudden beginning of the acceleration spoils the longitudinal emittance, since a low $|\phi_s|$ has to allow transverse stability. In this way one is forced to work in the non linear region of the RF field, with the beam pulse relatively long produced by the external bunching system; as a consequence the longitudinal emittance is multiplied by 3 in the first ten cells.

To solve this problem we have introduced an adiabatic bunch compressor, i.e. a section where ϕ_s is linearly ramped from -40^0 to -18^0. At the same time the modulation is increased so to avoid the parametric resonance:

$$0.4 \leq \frac{\sigma_t}{\sigma_l} \leq 0.6$$

and to maintain a nominal acceptance[*] higher than 1.2 mm mrad. These two requirements determine the law for *m*. In fig.4 the main RFQ parameters as a function of cell number are shown; the continuity around cell 41 (end of SRFQ1) is artificial.
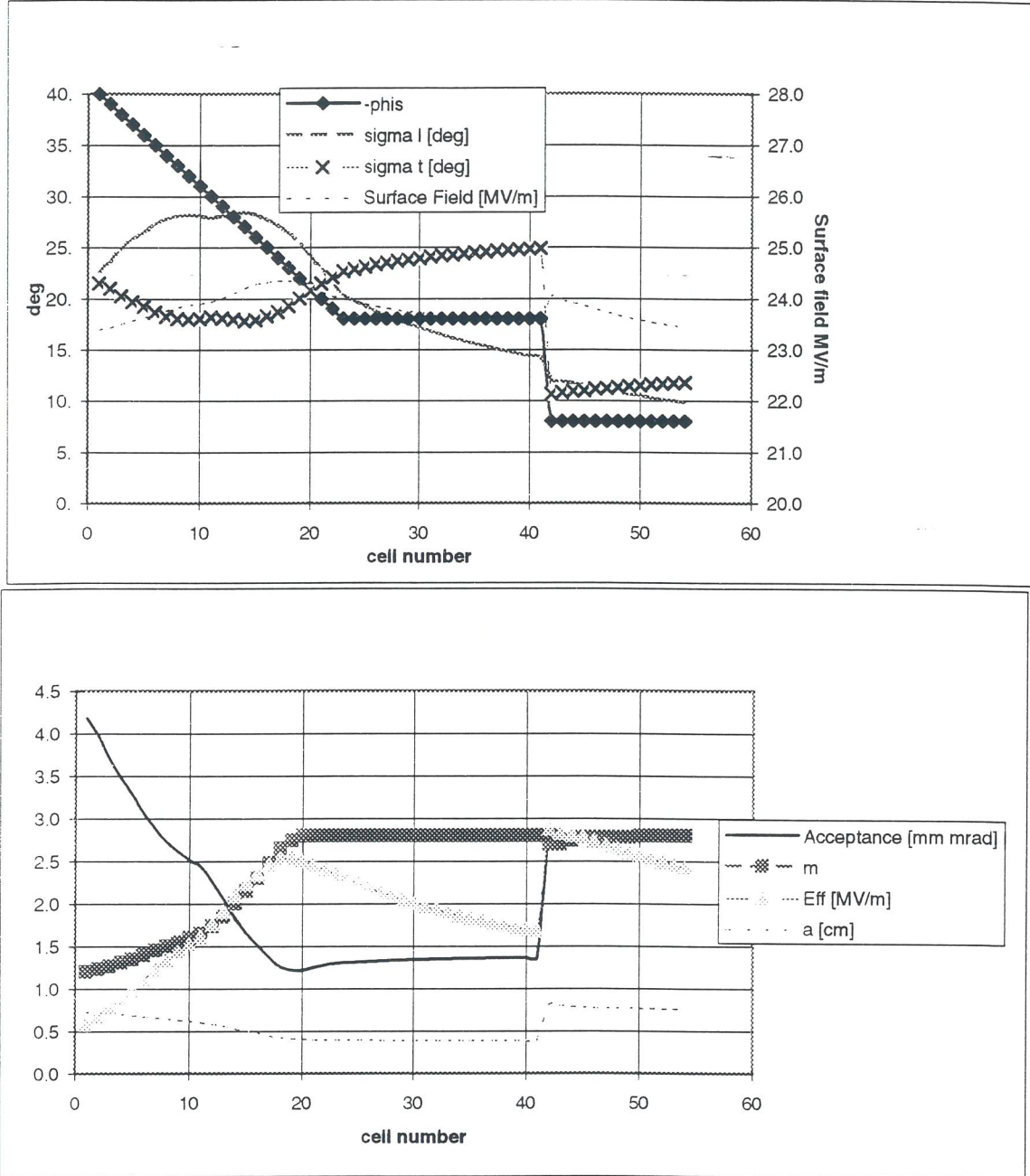

Fig .4 RFQ parameters as a function of the cell number.

---

[*] The nominal acceptance is the acceptance for a perfectly matched beam in a channel with adiabatically changing focusing functions. Unfortunately, due to our efficiency requirements, the focusing functions change rapidly respect to the betatron oscillations frequency. For this reason the effective acceptance has to be calculated "a posteriori" from simulations and is in our case around *0.9 mm mrad.*

At the entrance of the second RFQ the bunch is very short and $\phi_s = -8^0$ can be used. There is a longitudinal emittance increase but well within specifications. The nominal acceptance is more then *2.5 mm mrad* and can deal with the beam mismatch due to the drift space.

In Fig. 5 the beam envelopes in SRFQ1 and SRFQ2 are shown. In Fig.6 are plotted the input and output phase planes of the two RFQ's.

Table II SRFQ's nominal characteristics.

charge number	28
mass number	238
Platform Voltage	350 kV

	SRFQ1		SRFQ2		
	in	out	in	out	
Energy	41.2	341.7		578.3	keV/u
Beta	0.0094	0.0271		0.0352	
Voltage	150.0	150.0	280.0	280.0	kV
Length		134.7		76.3	cm
Ncell		41		13	
m	1.2	2.8	2.7	2.8	
a	0.7	0.4	0.8	0.8	cm
R0	0.80	0.80	1.53	1.53	cm
Phis	-40.0	-18.0	-8.0	-8.0	deg
Max. Surface field		24.3		24.0	MV/m
Stored energy		1.8		3.6	J

Total length	210.98 cm	(TTF	in the first QWR=	0.79)
Equivalent voltage	4.57 MV			
Average acceleration	2.16 MV/m			

The results of PARMTEQM [7] simulations are summarized in Fig. 7, where the survival rate after SRFQ1 and SRFQ2 are plotted as function of the input normalized emittance. The lower acceptance of SRFQ2 is due to the mismatching caused by the drift space between the two RFQs. In appendix A will be discussed a possible solution of this problem. In Fig. 7 is also plotted the final over initial emittance ratio (transverse and longitudinal). In our RFQs the transverse emittance increase is virtually zero, while the longitudinal emittance remains within specifications.

The same structure have been independently simulated with the program PROTON, developed at ITEP [8]. The results are in good agreement.
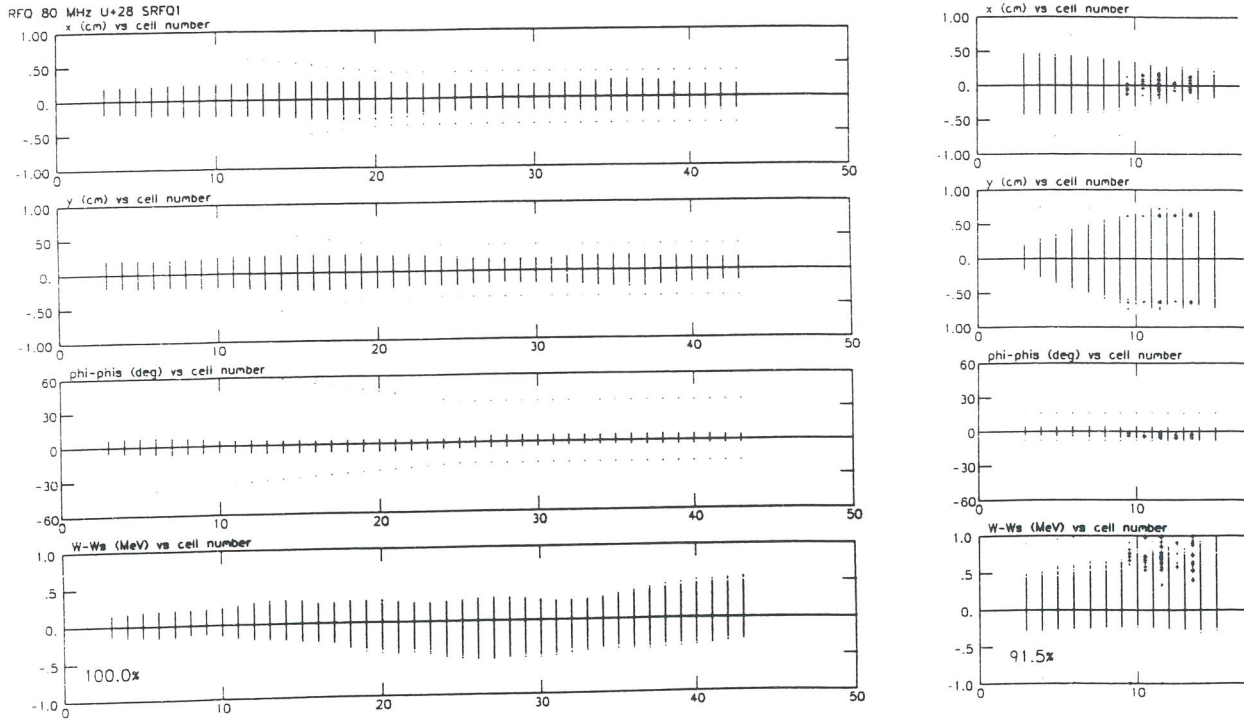
RFQ 80 MHz U+28 SRFQ1

x (cm) vs cell number

y (cm) vs cell number

phi-phis (deg) vs cell number

W-Ws (MeV) vs cell number

100.0%

RFQ 80 MHz U+28 SRFQ2

x (cm) vs cell number

y (cm) vs cell number

phi-phis (deg) vs cell number

W-Ws (MeV) vs cell number

91.5%

Fig.5 . Beam envelopes in the RFQ's.

phase-space projections at input of cell 3

x-xp (cm-radian)

y-yp (cm-radian)

dphi-dw (deg-mev)

phase-space projections at output of cell 15

x-xp (cm-radian)
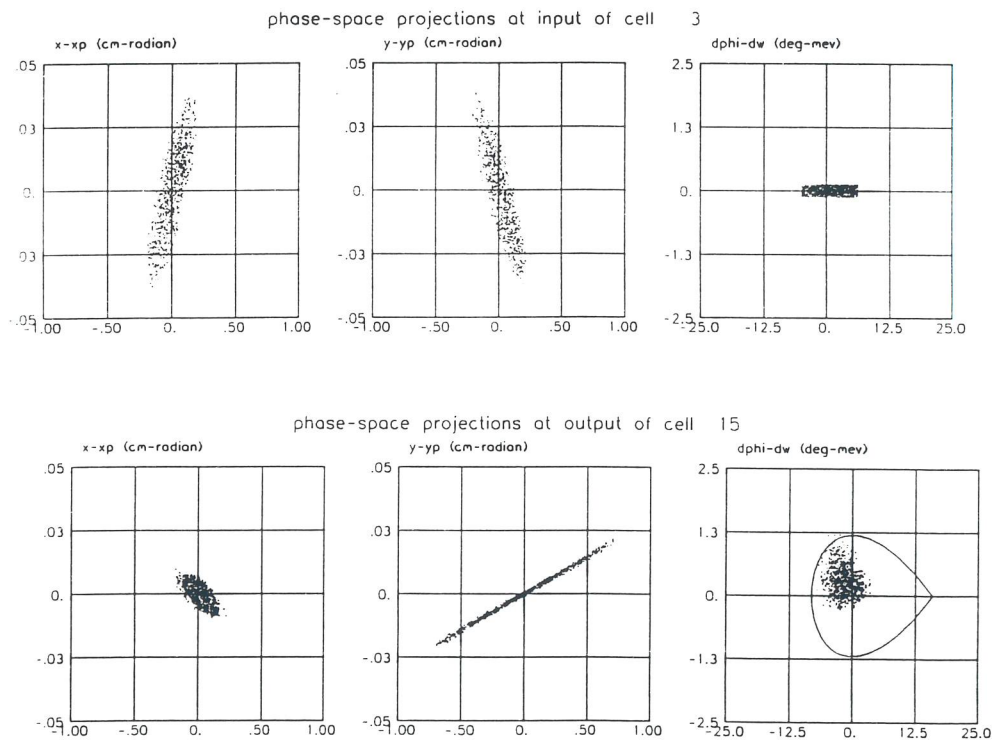
y-yp (cm-radian)

dphi-dw (deg-mev)

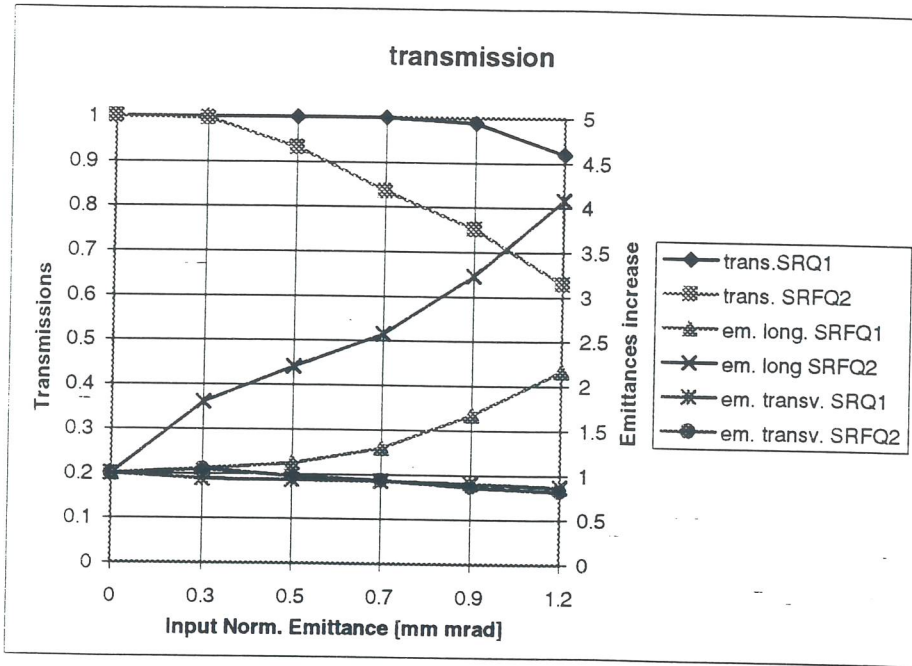*Fig 6* Phase space at RFQ section input and output.

Fig .7 Transmission rate after SRFQ1 and SRFQ2 as a function of the input normalized emittance. Longitudinal and Transverse relative emittance increase with the same dependence.

In table III the longitudinal emittance for our design (in various stages) is compared with the emittance of existing machines, namely GSI Unilac Injector [10] and ANL Positive Ion Injector [9]. Comparison between emittances simulated and measured with different methods is difficult and probably the accuracy is not more than 20÷50 %. Nevertheless it is possible to see that RFQ bunching (GSI) gives somewhat bigger emittances respect to external bunching (ANL and LNL). Emittances quoted by ANL are extremely low, but are in the region of what we can achieve with our design. There is a certain uncertainty in their transverse emittance: if we simulate a beam with 0.4 mm mrad we have their same longitudinal emittance.

Finally we mention that in table III is summarized the evolution of our injector design in the following four phases

- 3 SRFQ at 40 MHz followed by 3 SRFQ at 80 MHz;
- 3 SRFQ at 40 MHz followed by 12 QWR at 80 MHz;
- 2 SRFQ at 80 MHz followed by 8 QWR at 80 MHz;
- 2 SRFQ at 80 MHz with adiabatic bunch compressor followed by QWRs.

The improvement is evident, especially considering that the construction and phase locking of the 40 MHz RFQ is very problematic.

Table III Longitudinal emittances in existing injectors and for various designs of our one.

		Freq. [MHz]	A	Longitudinal Emittances				$\varepsilon_f/\varepsilon_i$
				deg keV/u	deg MeV	keV ns	ns keV/u	
Existing Facilities	pII (Pb) (ANL)	72.75	208	8.06	1.676	64	0.308	
	pII(Si)	72.75	30	31.43	0.943	36	1.200	
	IH Unilac (GSI)	108	238	70	16.66	428	1.800	2.9
	RFQ unilac	108	238	24	5.7	147	0.616	-
40 MHz	srfq input	40	238	1.47	0.35	24	0.102	-
	srfq (500keV/u)	40	238	4.62	1.1	76	0.321	3.1
	srfq(1.2MeV/u)	80	238	21.01	5	174	0.729	7.1
	srfq+qwr	80	238	11.76	2.8	97	0.408	4.0
80 MHz	srfq input	80	238	2.94	0.7	24	0.102	-
	srfq (500keV/u)	80	238	18.07	4.3	149	0.627	6.1
with adiab. compress.	srfq input	80	238	4.81	1.145	40	0.167	-
	srfq (500keV/u)	80	238	10.50	2.5	87	0.365	2.2
	NewInj (0.95MeV/u)	80	238	14.71	3.5	122	0.511	3.1

total emittances (=5*rms or 4*FWHH) quoted

for GSI and our cases normalized transverse emittance=0.5 mm mrad

5. LOW ENERGY BEAM TRANSPORT LINE (LEBT).

The ECR source is located above an HV platform, constructed on a concrete stand. The ECR beam plane is about *5 m* above the RFQ ALPI plane. The Low Energy Beam Transport line (LEBT) is composed by:
1. the platform beam transport, with charge state analysis and electrostatic tube;
2. the achromatic bend line;
3. the RFQ line, with transverse matching and bunching elements.

The beam is extracted by a *10-20 kV* voltage and analyzed in using a *90 deg, 0.5 m* bending radius magnet. Additional focusing is given by two einzel lenses, one before the dipole (to increase the angular acceptance) and one after the analysis waist to match the beam to the accelerating tube.

After the column the beam is transported to the RFQ input line with an achromatic U bend, so to make the transverse beam characteristics insensitive to HV fluctuation and energy modulation introduced by a possible *5 MHz* buncher on the platform. The U bend is almost vertical, with a slope of *20 deg*. This angle cause an emittance increase if the beam after the column has not cylindrical symmetry. But the focusing elements chosen on the platform should guarantee a symmetrical beam. In Fig.9 the beam envelopes and the dispersion function in the bend region are shown. Details about this line are in ref. [11]. In Table IV a preliminary dipoles and quadrupoles specification list is shown.
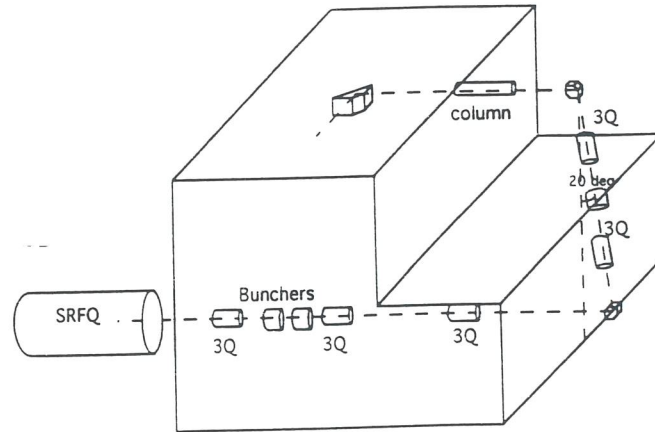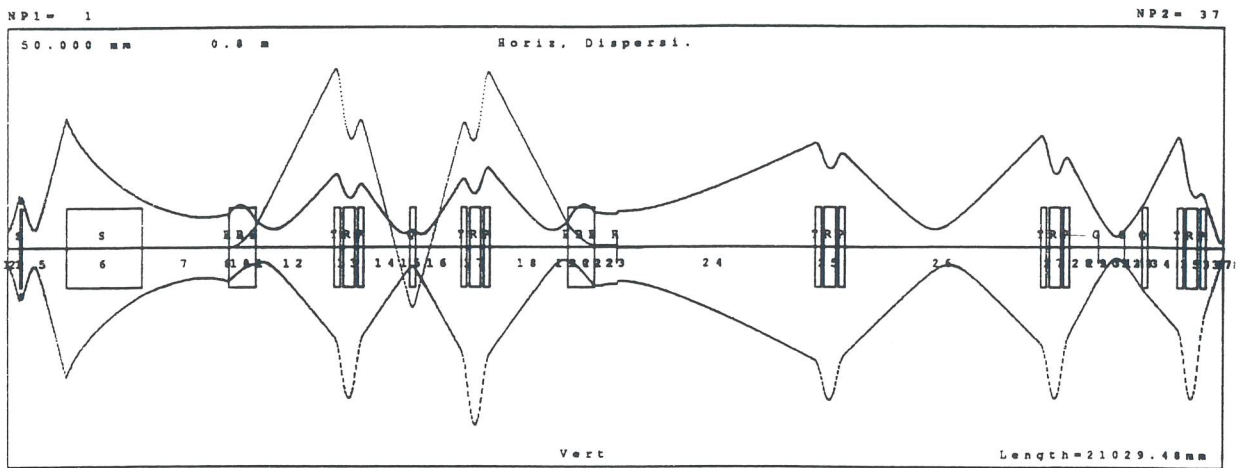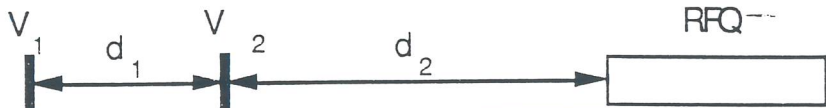
Fig 8 Sketch of the input line.

Fig 9. Beam envelopes in the input line.

Table IV Dipoles and qudrupoles characteristics

Dipoles	Bending radius	300	mm
	Bending angle	90	deg
	Focusing angle	28.8	deg
	Max. Field	1	T
	Gap	40	mm
Quadrupoles	Max. Tip Field	0.5	T
	Bore diameter	100	mm
	Max. Gradient	10	T/m
Triplet	Eff. lengths	100+50+200+50+100	mm
Singlet	Eff. length	200	mm

Last the beam is prepared for the RFQ. In table V the geometries for three different configurations are shown: a single *80 MHz* buncher, two double drift double frequency systems *80-160 MHz* and *40-80 MHz* respectively. Effective voltages (including transit time factor) and distances are calculated so to optimize the capture in the SRFQ1 phase and energy width acceptance [12].

Table V Bunching schemes before the SRFQ.

Beam at RFQ input	pulse width	±6	deg (80 MHz)
	energy modulation	±0.55	keV/u
Single buncher	80 MHz	V=4.7 kV	d=730 mm
Double drift and double frequency	80-160 MHz	V_1=3.6 kV	d_1=460 mm
		V_2=-1.92 kV	d_2=1730 mm
	40-80 MHz	V_1=3.6 kV	d_1=766 mm
		V_2=-1.72 kV	d_2=3293 mm

In Fig . 10 the input and output phase spaces for the RFQs after the *160-80 MHz* bunching are shown . The transmission in this case is 65 %.
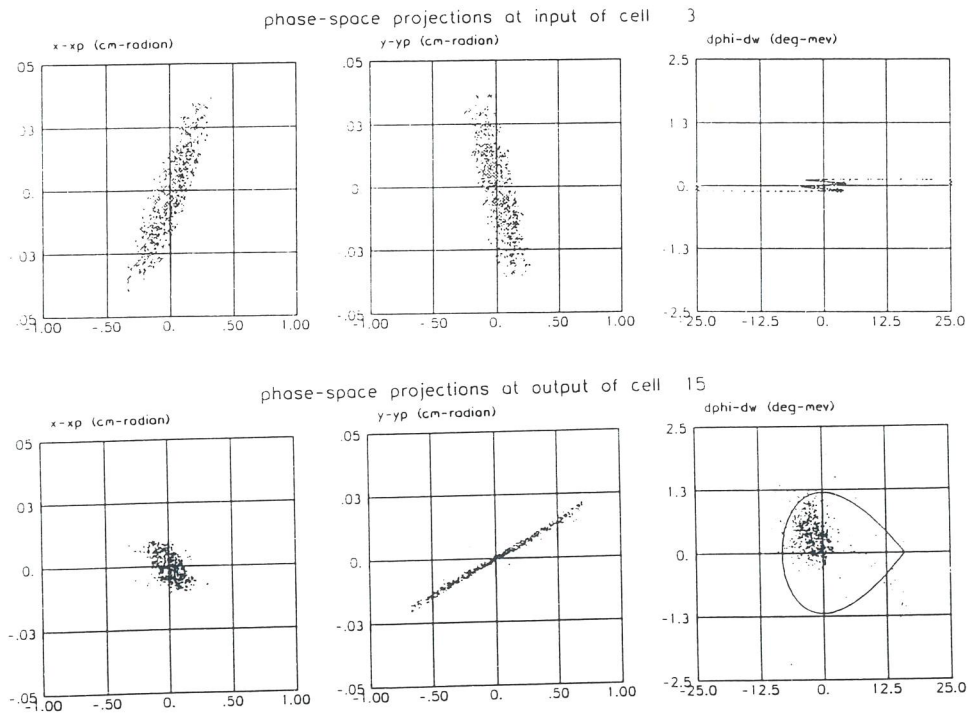

Fig 10. RFQ input and output phase space using a double drift double frequency buncher.

6. THE QWR'S AND THE MEDIUM ENERGY BEAM TRANSFER LINE (MEBT)

After the RFQ the beam is accelerated by eight QWR's located in two cryostats. Resonators and cryostats the same as in ALPI low energy section (possibly $\beta_0 = .050$, instead of $\beta_0 = .055$), but focusing is stronger, with a doublet before each cryostat instead of a triplet before each two. This increase of lenses number is necessary to overcome the RF defocusing, that is stronger at low energy; a compact configuration, with doublets instead of triplets and without diagnostics boxes, is necessary to keep the bunch length short.

It has to be noted that the accelerating field is limited to *3 MV/m* by beam dynamics considerations, at least in the first cavities (these resonators can exceed *4 MV/m*). This allows space for the specific optimization of each beam. In Fig. 11 are shown the beam envelopes for the U^{+28}. The last cavity of the first cryostat uses $\phi_s = 20^0$ (longitudinally defocusing) to have a regular phase envelope.
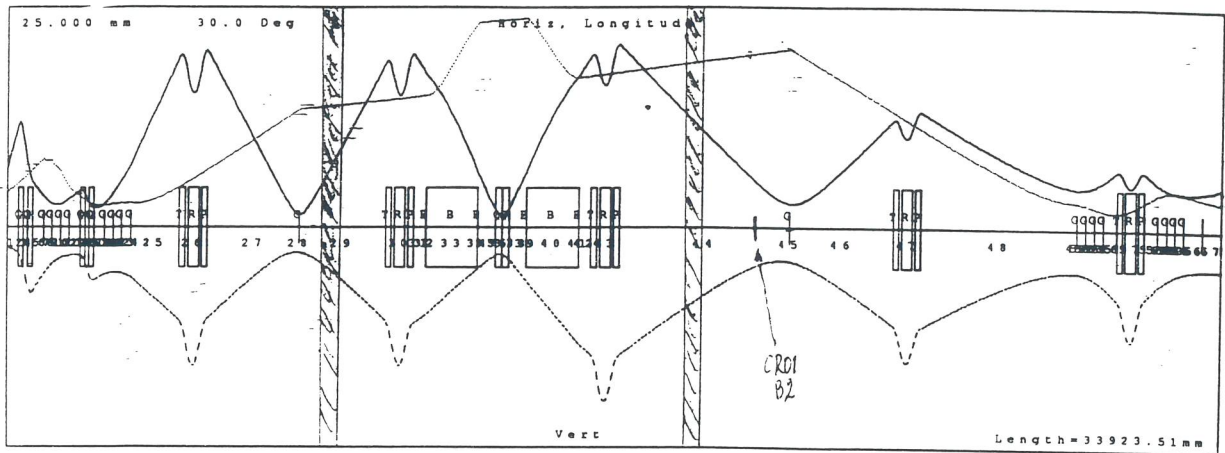

Fig .11 Beam envelopes in the QWR's region.

The new injector is completed by the line MEBT, that matches the beam into ALPI (in the three degrees of freedom) [11]. The line is composed by an achromatic L bend (identical to ALPI L bends), two (ALPI) triplets and two bunchers. The transverse focusing in the ALPI branch of MEBT is provided by the existing lenses. The two bunchers, operating at 80 MHz, are located in the beam waists before and after the L bend. The effective voltage in the bunchers is below *100 kV*, so that room temperature cavities are possible*[4].

---

* The Shunt impedance calculated with SUPERFISH (Cu room themperature) is 3.7 Mohm, corresponding to 2.7 kW dissipated (CW). A further optimization, with the freedom possible in a normal conducting geometry, and possibly the use of four gaps, should make possible the use of a 2.5 kW amplifier.

7. CONCLUSIONS

A nominal design for the New ALPI injector, based on two SRFQs and eight QWRs, has been determined; the input line, the SRFQs and the QWRs have been simulated with well proved codes, showing that all the specifications can be met. The amount of technological risk seems reasonable and well distributed between the various subsystems. In particular the use of compact 80 MHz SRFQs (possible with a sophisticated beam dynamics design) and of already developed QWRs are key points for the feasibility of the project. The design is therefore mature for SRFQ's prototyping and for the construction of the complex.

In the appendixes we show some alternatives and possible improvements that are worth of discussion, but do not interfere with the parameters given for SRFQ resonators R&D.

8. ACKNOWLEDGMENTS.

My thanks to A. Lombardi and G. Bisoffi, with whom in these two years we had day by day discussions in the intersection areas of interest for the determination of this superconducting RFQ concept; we share the hope and the engagement to built the injector within the established schedule.

The collaboration with ITEP (Moscow) and the visits of A.Kolomiets, S.Yaramishev and A. Balabin have given an indispensable contribution to the clarification of important points of this concept. M.Comunian and X.L.Guan (IAE, Beijin), with their work on code developement, have made possible systematic simulations.

9. REFERENCES.

1. M.Cavenago and G.Bisoffi "Commissioning of the ECR source Alice" NIM A328(193) p.262-265, and M.Cavenago "Selection of charge from the ECR Alice without forming a Waist", NIM, A328(1993),266-269.
2. A.Pisent, G.Fortuna "Ottica delle linee per la Terza Sala Sperimentale", LNL-INFN(REP) 101/95
3. G.Bisoffi, P.Favaron, A.Lombardi, A.Pisent, R.Tovo "The Positive Ion Injector for ALPI", presented to the 7th International Conference on Heavy Ion Acceleration Technology, Canberra.
4. A.Facco NIM and Private Communications
5. I.Ben-Zvi, A.Lombardi "Design of a Superconducting RFQ resonator" Particle Accelerators 35 (1991) 177.
6. A.Balabin "Optimization of the accelerating field in a RFQ with high modulation: calculation of the surface and accelerating field for the actual geometry", LNL internal note (1994).
7. A.Kolomiets "Summary of beam dynamics simulation results for the new injector", LNL internal note (1995).
8. PARMTEQ

9. L.M.Bollinger et al. "First operational experience with the positive-ion injector of ATLAS", NIM A328 (1993) p. 221-230.

10. J.Klabunde "The High Charge State Injector for GSI", 1992 Linear Accelerator Conference Proceedings, AECL-10728, p.570.

11. A. Pisent, S.Yaramishev "Beam Transport Lines for New Positive Ion Injector" LNL internal note (1996).

12. K.R. Crandall "Optimum Buncher Parameters for Small Beam Currents" LANL internal note (1967).

13. G.Amendola, J.M.Quesada, M.Weiss and A.Pisent. "Beam Dynamics studies for the CERN Lead-Ion RFQ" Proceedings of the third European Accelerator Conference, Berlin 1992, p.973

APPENDIX A End cell and cross-over matching.

The RFQ electrodes are generally terminated at the end of a cell, i.e. where the profiles are parallel to beam axis (Fig. A1). This approach is followed by LANL designer and by everybody using PARMTEQ and related codes, at CERN, GSI, Frankfurt and LNL (Lead Ion injector RFQ).

In this way the electrodes are cut in a position where the electric field is completely transverse, with some advantages for the predictability of the field in the transition region; on the other hand doing this the strength of the alternating gradient focusing at the end of SRFQ1 is $B\,cos(-\phi_s)$ on one plane and $B\,cos(\pi-\phi_s)$ on the other, i.e. in general the envelopes have neither minimum nor a maximum dimensions. In the following space the beam diverges in both planes and enters mismatched into SRFQ2. The effect is clear in Fig. 5, 6 and 7, with envelopes, phase spaces and resulting transmissions.

The mismatch after a drift space is minimized if the beam is at a "cross-over" before the drift, i.e. if the envelopes have a minimum on one plane an a maximum on the other. This condition can be fulfilled by cutting the last SRFQ1 cell and the first SRFQ2 cell as shown in Fig.A1.

This approach was suggested by A.Balabin and A. Kolomiets and turned out to be very effective. In Fig. A2 the analogous of Fig. 7 in the presence of cross-over matching is shown. Before choosing the implementation of this cut we shall do some 3D Poisson calculations of the RFQ end, in the presence of the tank wall, so to calculate the fields where the usual assumption of a periodic modulation is not valid. In particular first order effects like the effective length of the last cell (considered as a quadrupole) and the transit time factor for the longitudinal field in the gap between electrodes and tank wall have to be evaluated.
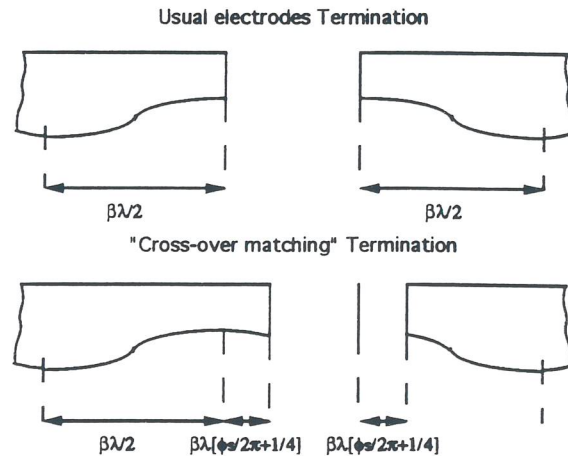

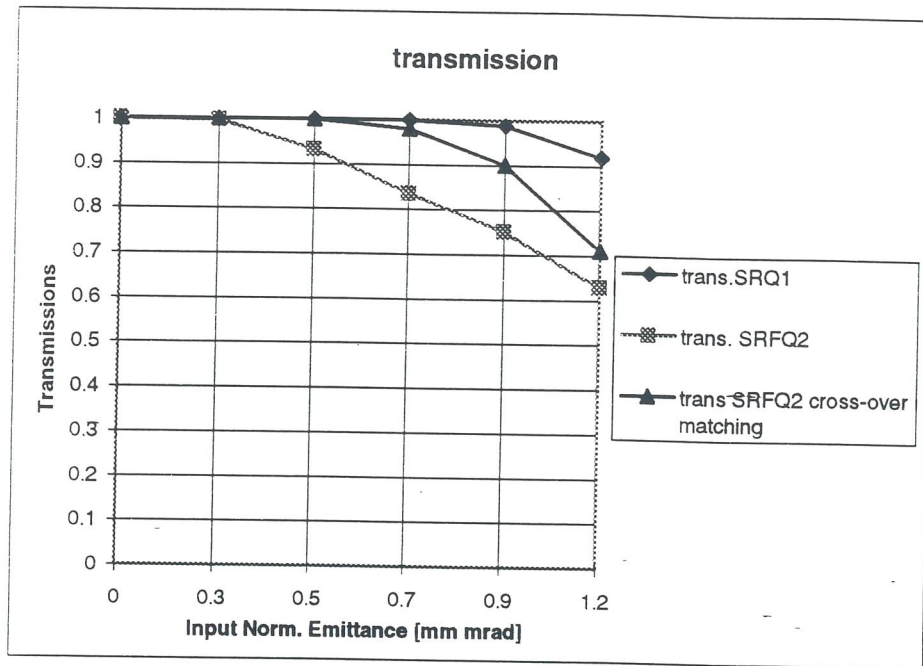Fig . A1 usual (LANL) and "cross-over" (ITEP) termination of the electrodes.

transmission

Fig . A2 Transmission curves for usual and "cross-over" cut of the electrodes..

APPENDIX B. Different choices for the input energy.

We present in this appendix two options for the input energy different from the nominal choice (corresponding to 350 kV platform voltage):

- injection into the RFQ directly after 20 kV of extraction voltage;
- injection after 150 kV of platform voltage.

With the first option the bunching can be operated inside the RFQ, with an efficiency above 95%. The second option makes more reliable the HV system of the platform (an investigation in this sense has been recommended by the review committee).

a Adiabatic Bunching RFQ

The possibility of an adiabatic bunching is one of the main features of RFQ accelerators: the acceleration parameters are changed slowly from cell to cell, starting from $\phi_s=-90^0$ and $m=1$. A certain number of cells (generally more then hundred) with very low accelerating efficiency is necessary for this process, so that for our nominal case ($\beta=.01$ at input) the RFQ becomes prohibitively long, and the choice of an external bunching is necessary.

We consider instead here the case of a direct injection after 20 kV of ECR extraction voltage ($\beta=.0022$). The technique and the algorithms are the same used for our RFQ built for CERN, but with a longer shaper section, so to have higher capture and lower longitudinal emittance[14]. In Fig. B1 the beam envelopes and the output emittances are shown. The result is a scenario (as shown in table BI) with three RFQs, a capture above 95% and a final emittance of 1.5 ns kev/u. This results is possible only if at the transition before SRFQ1 (second RFQ) the "cross-over" described in appendix A is implemented.

This solution is rather attractive, even if the construction of a third SRFQ can cause budget and time schedule problems. Moreover an RFQ with such a small R_0 will have severe mechanical tolerances, difficult to fulfill in a superconducting resonator.

Table BI RFQ parameters with RFQ bunching after the 20kV extraction voltage.

	SRFQ buncher		SRFQ 1		SRFQ 2		
	in	out	in	out	in	out	
Energy	2.35	168.8		423.4		672.0	keV/u
	0.56	40.18		100.77		159.93	MeV
Beta	0.0022	0.0190		0.0302		0.0380	
Voltag e	93	93	200.0	200.0	290.0	290.0	kV
Length		148.5		128.1		83.3	cm
Ncell		167		29		13	
m	1	2.6	1.2	2.8	2.8	2.8	
a	0.5	0.288	0.9	0.5	0.8	0.8	cm
R0	0.5	0.5	1.00	1.00	1.60	1.60	cm
Phis	-90	-25	-40.0	-18.0	-8.0	-8.0	deg
Max. Sur. Field		25		25.4		23.7	MV/m
Stored energy		0.51		3.1		4.2	J

Total length	359.96 cm	(TTF 1st QWR= 0.88)
Equivalent voltage	5.69 MV	
Average acceleration	1.58 MV/m	
Es/Ea	16.0	

DESIGN ,FREQ= 80.00 MHZ, Q= 1.0,WI= 0.020,WF= 0.89 I= 0.0MA, RC=-0.37500
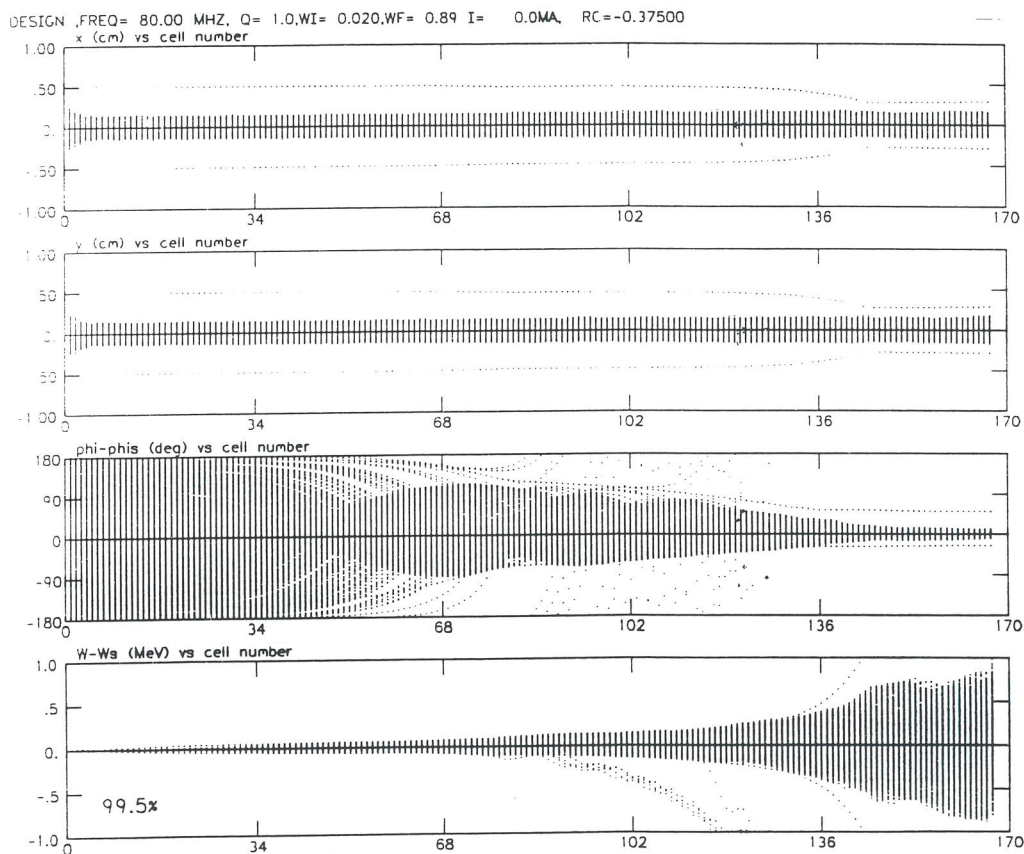

Fig . B1 Beam envelopes and output emittance of the bunching RFQ.

b. Platform voltage of 150 kV

The HT voltage of the platform can be decreased to 150 kV by increasing the RFQ length of about 10 cm respect to the nominal case. Tables BII and BIII show two scenarios, with a longer SRFQ1 and SRFQ2 respectively. In the first case we keep the SRFQ2 design (this RFQ will be built first) and the transition energy, but the compatibility of a longer SRFQ1 with the e-beam welding procedure has to be checked. In the second case the length of the SRFQ's is more comparable and construction problems seem excluded.

The LEBT transport has to be reconsidered with the bigger geometrical emittance; moreover the possible bunching systems, summarized in Table BIII, are very compact and the optics of the matching part has to be modified.

In Fig. B2 we show the SRFQ1 and SRQ2 acceptance, that is lower then in the nominal case.

Table BII RFQ parameters for 150kV platform voltage and SRFQ1 longer than the nominal one.

	SRFQ 1		SRFQ 2		
	in	out	in	out	
Energy	17.6	330.5		566.6	keV/u
	4.20	78.65		134.86	MeV
Beta	0.0062	0.0266		0.0349	
Voltage	140.0	140.0	280.0	280.0	kV
Length		145.2		75.3	cm
Ncell		51		13	
m	1.2	2.8	2.7	2.8	
a	0.68	0.36	0.81	0.76	cm
R0	0.75	0.75	1.53	1.53	cm
Phis	-40.0	-18.0	-8.0	-8.0	deg
Max. Surface field		24.5		24.1	MV/m
Stored energy		1.7		3.5	J

Total length   220.49 cm   (TTF in first QWR=   0.78)
Equivalent voltage   4.67 MV
Average acc.   2.12 MV/m
Es/Ea   11.6

Table BII RFQ parameters for 150kV platform voltage and SRFQ2 longer than the nominal one.

	SRFQ 1		SRFQ 2		
	in	out	in	out	
Energy	17.6	311.9		569.1	keV/u
Beta	0.0062	0.0259		0.0350	
Voltage	140.0	140.0	260.0	260.0	kV
Length		135.4		86.0	cm
Ncell		49		15	
m	1.2	2.8	2.7	2.8	
a	0.68	0.36	0.72	0.67	cm
R0	0.75	0.75	1.37	1.37	cm
Phis	-40.0	-18.0	-8.0	-8.0	deg
Max. Surface field		24.5		24.7	MV/m
Stored energy		1.6		3.5	J

Total length	221.38 cm	(TTF in first QWR=	0.78
Equivalent voltage	4.69 MV		
Average acc.	2.12 MV/m		
Es/Ea	11.7		

Table V Bunching schemes before the SRFQ.

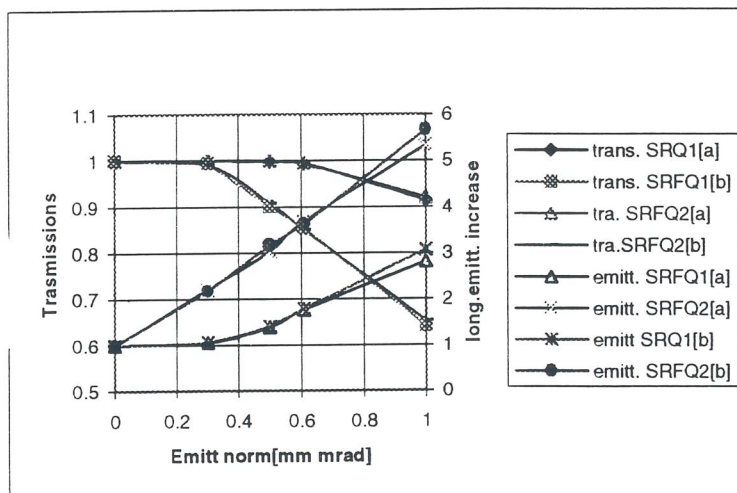| Beam at RFQ input	pulse width	±7.5	deg (80 MHz)
	energy modulation	±0.39	keV/u
Double drift and double frequency	80-160 MHz	V_1=2.8 kV	d_1=211 mm
		V_2=-1.69 kV	d_2=712 mm
	40-80 MHz	V_1=2.8 kV	d_1=334 mm
		V_2=-1.40 kV	d_2=1377 mm

Fig . B2 Transmission curves for the two options ([a] longer SRFQ1 and [b] longer SRFQ2) with 150kV platform voltage. The behaviour in SRFQ2 can be improved according to Appendix A.